

NEUMANN SERIES IN GMRES AND ALGEBRAIC MULTIGRID SMOOTHERS

STEPHEN THOMAS*, ARIELLE CARR†, PAUL MULLOWNEY*, RUIPENG LI‡, AND KASIA ŚWIRYDOWICZ§

Abstract. Neumann series underlie both Krylov methods and algebraic multigrid smoothers. A low-synchronization modified Gram-Schmidt (MGS)-GMRES algorithm is described that employs a Neumann series to accelerate the projection step. A corollary to the backward stability result of Paige et al. [1] demonstrates that the truncated Neumann series approximation is sufficient for convergence of GMRES under standard conditions. The lower triangular solver associated with the correction matrix $T_m = (I + L_m)^{-1}$ may then be replaced by a matrix-vector product with $T_m = I - L_m$. Next, Neumann series are applied to accelerate the classical Ruge-Stuben algebraic multigrid (AMG) preconditioner using either a polynomial Gauss-Seidel or incomplete ILU smoother. Here, the sparse triangular solver employed in the Gauss-Seidel and ILU smoothers is replaced by an inner iteration based upon matrix-vector products. Henrici’s departure from normality of the associated iteration matrices leads to a better understanding of these series. Additionally, connections are made between the (non)normality of the L and U factors and nonlinear stability analysis, as well as the pseudospectra of the coefficient matrix. Furthermore, re-orderings that preserve structural symmetry also reduce the departure from normality of the upper triangular factor and improve the relative residual of the triangular solves. To demonstrate the effectiveness of this approach on many-core architectures, the proposed solver and preconditioner are applied to the pressure continuity equation for the incompressible Navier-Stokes equations of fluid motion. The pressure solve time is reduced considerably without a change in the convergence rate and the polynomial Gauss-Seidel smoother is compared with a Jacobi smoother. Numerical and timing results are presented for Nalu-Wind and the PeleLM combustion codes, where ILU with iterative triangular solvers is shown to be much more effective than polynomial Gauss-Seidel.

1. Introduction. The purpose of the present work is to show the important role Neumann series play in MGS-GMRES and C-AMG smoothers. By revealing this structure and analyzing it, we devise ways to speed-up the GMRES+AMG solver in hypre [2]. The generalized minimal residual (GMRES) Krylov subspace method [3] is often employed to solve the large linear systems arising in high-resolution physics based simulations using the incompressible Navier-Stokes equations in fluid mechanics. Świrydowicz et al. [4] recently improved the parallel strong-scaling of the algorithm by reducing the MPI communication requirements to a minimum, while maintaining the numerical stability and robustness of the original algorithm. In order to achieve fast convergence of an elliptic solver, such as the pressure continuity equation, the classical Ruge-Stuben [5] algebraic multigrid (C-AMG, or simply AMG) solver is applied as a preconditioner. The low-synchronization MGS-GMRES iteration, Gauss-Seidel and ILU smoothers employ direct triangular solvers.¹ The triangular solve in GMRES is relatively small and local to each MPI rank. For Gauss-Seidel the coarse level matrices in the AMG V -cycle are distributed and some communication is required. Triangular solvers are, in general, difficult to implement in parallel on many-core architectures. In this study, the associated iteration matrices are replaced by truncated Neumann series expansions leading to polynomial-type smoothers. They result in a highly efficient and backward stable approach for Exascale class supercomputers.

Consider the large, sparse linear systems arising from the discretization of the incompressible Navier-Stokes pressure continuity equation [6]. In the present study, linear systems of the form $A\mathbf{x} = \mathbf{b}$ with A an $n \times n$ real-valued matrix, are solved with Krylov subspace methods using one V -cycle of the C-AMG algorithm as the preconditioner. Here, let $\mathbf{r}^{(0)} = \mathbf{b} - A\mathbf{x}^{(0)}$ denote the initial residual with initial guess $\mathbf{x}^{(0)}$. Inside GMRES, the Arnoldi QR algorithm is applied to generate an orthonormal basis for the Krylov subspace $\mathcal{K}_m(B)$ spanned by the columns of the $n \times m$ matrix, V_m , where $m \ll n$, and produces the $(m+1) \times m$ Hessenberg matrix, $H_{m+1,m}$, in the Arnoldi expansion such that

$$AV_m = V_{m+1}H_{m+1,m}.$$

In particular, the Arnoldi algorithm produces a QR factorization of $B = [\mathbf{r}^{(0)}, AV_m]$ and the columns of V_{m+1} form an orthogonal basis for the Krylov subspace $\mathcal{K}_{m+1}(B)$ [1]. The orthogonality of the columns determines the convergence of Krylov methods for linear system solvers. However, in finite-precision arithmetic, V_m may “lose” orthogonality and this loss, as measured by $\|I - V_m^T V_m\|_F$, may deviate

*National Renewable Energy Laboratory, Golden, Colorado

†Lehigh University, Bethlehem, PA

‡Lawrence Livermore National Laboratory, Livermore CA

§Pacific Northwest National Laboratory, Richland, WA

¹Note that the phrase *direct triangular solver* is used to differentiate between the iterative approximations versus the traditional forward and backward recurrences.

substantially from machine precision, $\mathcal{O}(\varepsilon)$, (see Paige and Strakos [7]). When linear independence is completely lost, the Krylov iterations may fail to converge. For example, the MGS-GMRES iteration will stall in this case, and this occurs when $\|S_m\|_2 = 1$, where the matrix $S_m = (I + U_m)^{-1}U_m$ was introduced in the seminal backward stability analysis of Paige et al. [1]. Here, U_m is the $m \times m$ strictly upper triangular part of $V_m^T V_m$.

The development of low-synchronization Gram-Schmidt and generalized minimal residual algorithms by Świrydowicz et al. [4] and Bielich et al. [8] was largely driven by applications that need stable, yet scalable solvers. Both the modified (MGS) and classical Gram-Schmidt with re-orthogonalization (CGS2) are stable algorithms for a GMRES solver. Indeed, CGS2 results in an $\mathcal{O}(\varepsilon)$ loss of orthogonality, which suffices for GMRES to converge. Paige et al. [1] show that despite $\mathcal{O}(\varepsilon)\kappa(B)$ loss of orthogonality, MGS-GMRES is backward stable for the solution of linear systems. Here, the condition number of the matrix B is given by $\kappa(B) = \sigma_{\max}(B)/\sigma_{\min}(B)$, where $\sigma_{\max}(B)$ and $\sigma_{\min}(B)$ are the maximum and minimum singular values of the matrix B , respectively.

An inverse compact WY (ICWY) modified Gram-Schmidt algorithm is presented in [4] and is based upon the application of a projector

$$P = I - V_m T_m V_m^T, \quad T = (V_m^T V_m)^{-1}$$

where V_m is again $n \times m$, I is the identity matrix of dimension n , and T_m is an $m \times m$ correction matrix. To obtain a one-reduce MGS algorithm, or one MPI global reduction per GMRES iteration, the normalization is delayed to the next iteration. The correction matrix T_m is obtained from the strictly lower triangular part of $V_m^T V_m$, denoted L_m . Note that because V_m has almost orthonormal columns, the norm of L_m is small, and T_m is close to I (here, the identity matrix of dimension m).

In this work, an alternative to computing the inverse of T_m via triangular solve is developed. A Neumann series expansion for the inverse of the lower triangular correction matrix, T_m , results in the ICWY representation of the projector P for the modified Gram-Schmidt factorization of the Arnoldi matrix B . This is written as

$$(1.1) \quad P = I - V_m T V_m^T, \quad T_m = (I + L_m)^{-1} = I - L_m + L_m^2 - \dots + L_m^p,$$

where the columns of L_m are defined by the matrix-vector products $V_{m-2}^T \mathbf{v}_{m-1}$. The sum is finite because the matrix L_m is nilpotent, as originally noted by Ruhe [9].

In this paper, a corollary to the backward stability result of Paige et al. [1] and Paige and Strakoš [7] is presented that demonstrates matrix-vector multiplication by $T_m = I - L_m$ in the projection step is sufficient for convergence of MGS-GMRES when $\|L_m\|_F^p = \mathcal{O}(\varepsilon^p)\kappa_F^p(B)$, where $p > 1$. A new formulation of GMRES based upon the truncated Neumann series for the matrix T_m is presented. In particular, the loss of orthogonality and backward stability of the truncated and MGS-GMRES algorithms are the same because of the above corollary. For extremely ill-conditioned matrices, the convergence history of the new algorithm has been found to be identical to the original GMRES algorithm introduced by Saad and Schultz [3]. In particular, convergence is achieved when the norm-wise relative backward error reaches machine precision (NRBE); see Section 4 for more details. For this reason, Paige and Strakoš [7] recommended that the NBRE be applied as the stopping criterion.

A polynomial Gauss-Seidel iteration can also be interpreted with respect to the degree- p Neumann series expansion as described in the recent paper by Mullowney et al. [10]. Given the regular matrix splitting $A = M - N$, $A = D + L + U$, $M = D + L$ and $N = -U$,² the polynomial Gauss-Seidel iteration is given by

$$\mathbf{x}^{(k+1)} := \mathbf{x}^{(k)} + (I + D^{-1}L)^{-1} D^{-1}\mathbf{r}^{(k)} = \mathbf{x}^{(k)} + \sum_{j=0}^p (-D^{-1}L)^j D^{-1}\mathbf{r}^{(k)}$$

For the ILU factorization [11], the $L = I + L_s$ factor has a unit diagonal and strictly lower triangular part L_s . Thus, the inverse L^{-1} may be expressed as a Neumann series and, with L_s nilpotent, this is a

²Note that by convention, this matrix splitting is written such that L is the strictly lower triangular part of A , and U is the strictly upper triangular part. The matrices L and U in Gauss-Seidel smoother are different from the those used in Gram-Schmidt projection in (1.1).

finite sum. Similarly, for the strictly upper triangular factor U_s such that $U = I + U_s$, after either row or row/column scaling, the inverse can be written as a Neumann series, as follows

$$(I + U_s)^{-1} = I - U_s + U_s^2 - \dots$$

Furthermore, when $\|U_s^p\|_2 < 1$, for $p \geq 1$ the series converges. In the present study, the above iterations are applied as smoothers when constructing a C-AMG preconditioner.

In [12], a method for scaling the U factor to form $U = I + U_s$ in order to mitigate a high degree of non-normality and condition number is proposed. In general, fast convergence of the Jacobi iteration can then be expected [13] when iteratively computing the triangular solution, thus avoiding the comparatively high cost on the GPU of a direct triangular solve. Here, the analysis in [12] is extended and theoretical upper bounds on the departure from normality [14] of a (row and/or column) scaled triangular matrix are provided. In the case of nonsymmetric coefficient matrices, reordering prior to scaling may be employed to enforce a symmetric sparsity pattern. Following the analysis in [11], an empirical relationship between the drop tolerance and fill level used when computing an incomplete LU factorization and the subsequent departure from normality of the triangular factors following row and/or column scaling is established.

An additional contribution of our paper is to combine three different Neumann series to create fast and robust solvers. The time to solution is the most important metric versus the number of solver iterations taken in fluid mechanics simulations. The low-synchronization MGS-GMRES may take a larger number of iterations at little or no extra cost if the preconditioner is less expensive. However, the triangular solvers employed by smoothers are not efficient on multi-core architectures. Indeed, the sparse matrix-vector product (SpMV) is 25–50× faster on GPU architectures [13]. This observation prompted the introduction of polynomial AMG smoothers in [10], which significantly lowers the cost of the V -cycle.

The paper is organized as follows. Low synchronization and generalized minimal residual algorithms are discussed in Section 2. A corollary to Paige et al. [1] in Section 3 establishes that $T_m = I - L_m$ is sufficient for convergence. In Section 4, a variant of MGS-GMRES is presented that uses this T_m . Section 5 describes recent developments for hypre on GPUs. The polynomial Gauss-Seidel and ILU smoothers are then introduced in Section 5 where it is shown that pivoting leads to rapid convergence of iterative triangular solvers. The departure from normality of the factors can also be mitigated by either row or row and column scaling via the Ruiz algorithm, thus avoiding divergence of the iterations.

Notation Lowercase bold letters denote a column vector and uppercase letters are matrices (e.g., \mathbf{v} and A , respectively). a_{ij} represents the (i, j) scalar entry of a matrix A , and \mathbf{a}_j denotes the j^{th} column of A . Where appropriate, for a matrix A , A_j is the j -th column. Superscripts indicate the approximate solution (e.g., $\mathbf{x}^{(k)}$) and corresponding residual (e.g., $\mathbf{r}^{(k)}$) of an iterative method at step k . Throughout this paper, we will explicitly refer to *strictly upper/lower triangular matrices* and use the notation U_k (or L_k) and U_s (or L_s).³ Vector notation indicates a subset of the rows and/or columns of a matrix; e.g., $V_{1:k+1,1:k}$ denotes the first $k+1$ rows and k columns of the matrix V and the notation $V_{:,1:k}$ represents the entire row of the first k columns of V . $H_{m+1,m}$ represents an $(m+1) \times m$ matrix, and in particular H refers to a Hessenberg matrix. In cases where standard notation in the literature is respected that may otherwise conflict with the aforementioned notation, this will be explicitly indicated.

2. Low-Synchronization Gram-Schmidt Algorithms. Krylov linear system solvers are often required for extreme scale physics simulations on parallel machines with many-core accelerators. Their strong-scaling is limited by the number and frequency of global reductions in the form of `MPI_AllReduce` and these communication patterns are expensive. Low-synchronization algorithms are designed such that they require only one reduction per iteration to normalize each vector and apply projections.

A review of compact WY Gram Schmidt algorithms and their computational costs is given in [8]. The ICWY form for MGS is the lower triangular matrix $T_k = (I + L_k)^{-1}$ and was derived in Świrydowicz et al. [4]. Here, I denotes the identity matrix and L_k is strictly lower triangular. Specifically, these algorithms batch the inner-products together and compute one row of L_k as

$$(2.1) \quad L_{k-1,1:k-2} = (V_{k-2}^T \mathbf{v}_{k-1})^T.$$

³We note that the distinction between these two notations is crucial. For U_k , the size of the strictly upper triangular matrix changes with k , whereas the size of U_s remains fixed.

The resulting ICWY projector P is given by

$$P = I - V_{k-1} T_{k-1} V_{k-1}^T, \quad T_{k-1} = (I + L_{k-1})^{-1}$$

The implied triangular solve requires an additional $(k-1)^2$ flops at iteration $k-1$ and thus leads to a slightly higher operation count compared to the original MGS algorithm. The matrix-vector multiply in (2.1) increases the complexity by mn^2 ($3mn^2$ total) but decreases the number of global reductions from $k-1$ at iteration k to only one reduction when combined with the lagged normalization of a Krylov vector.

3. Loss of Orthogonality. When the Krylov vectors are orthogonalized via the finite precision MGS algorithm, and their loss of orthogonality is related in a straightforward way to the convergence of GMRES. In particular, orthogonality among the Krylov vectors is effectively maintained until the norm-wise relative backward error approaches the machine precision as discussed in Paige and Strakoš [7]. In this section, a corollary to Paige et al. [1] establishes that $T_k = (I + L_k)^{-1} = I - L_k + \mathcal{O}(\varepsilon^2)\kappa^2(B)$, where $B = [\mathbf{r}^{(0)}, AV_k]$ for the ICWY MGS formulation of the Arnoldi expansion.

Let A be an $n \times n$ real-valued matrix, and consider the Arnoldi factorization of the matrix B . After k steps, in exact arithmetic, the algorithm produces the factorization

$$AV_k = V_{k+1} H_{k+1,k}, \quad V_{k+1}^T V_{k+1} = I_{k+1}$$

where $H_{k+1,k}$ is an upper Hessenberg matrix. When applied to the linear system $A\mathbf{x} = \mathbf{b}$, assume $\mathbf{x}^{(0)} = 0$, $\mathbf{r}^{(0)} = \mathbf{b}$, $\|\mathbf{b}\|_2 = \rho$ and $\mathbf{v}_1 = \mathbf{b}/\rho$. The Arnoldi algorithm produces an orthogonal basis for the Krylov vectors spanned by the columns of the matrix V_k . Following the notation in [1], the notation \bar{A}_k is employed to represent the computed matrix in finite-precision arithmetic with k columns, and \tilde{A}_k to represent the properly normalized matrix with k columns. We refer the reader to [1] for more details on these definitions. Consider the computed matrix \bar{V}_k with Krylov vectors as columns. The strictly lower triangular matrix \bar{L}_k is obtained from the loss of orthogonality relation

$$\bar{V}_k^T \bar{V}_k = I + \bar{L}_k + \bar{L}_k^T.$$

Let us first consider the lower triangular solution algorithm for T_k where the elements of L_k appear in the correction matrix T_k , along with higher powers of the inner products in the Neumann series.

A corollary to the backward stability results from Paige and Strakoš [7], and Paige et al. [1] is now established, namely that the Neumann series for T_k may be truncated according to

$$T_k = (I + \tilde{L}_k)^{-1} = I - \tilde{L}_k + \mathcal{O}(\varepsilon^2)\kappa^2(B).$$

The essential result is based on the QR factorization of the matrix

$$B = [\mathbf{r}^{(0)}, AV_k] = V_{k+1} [\mathbf{e}_1 \rho, H_{k+1,k}].$$

A bound on the loss-of-orthogonality given by

$$\|I - \tilde{V}_{k+1}^T \tilde{V}_{k+1}\|_F \leq \kappa([\mathbf{r}^{(0)}, AV_k]) \mathcal{O}(\varepsilon),$$

and the derivation of this result allows us to find an upper bound for $\|\tilde{L}_k\|_F^p$.

The upper triangular structure of the loss of orthogonality relation is revealed to be

$$\tilde{U}_k = (I - \tilde{S}_k)^{-1} \tilde{S}_k = \tilde{S}_k (I - \tilde{S}_k)^{-1}$$

and it follows that $\tilde{L}_k = \tilde{U}_k^T$,

$$\begin{aligned} I - \tilde{S}_k^T &= I - \tilde{L}_k (I + \tilde{L}_k)^{-1} \\ &= I - \tilde{L}_k (I - \tilde{L}_k + \tilde{L}_k^2 - \tilde{L}_k^3 + \dots) \\ &= (I + \tilde{L}_k)^{-1} \end{aligned}$$

where $\tilde{U}_k = \tilde{L}_k^T$ is the strictly upper triangular part of $\tilde{V}^T \tilde{V}$. It then follows immediately, that a bound on the loss of orthogonality is given by

$$\sqrt{2} \|\tilde{V}_k^T \tilde{\mathbf{v}}_k\|_2 \leq \|I - \tilde{V}_k^T \tilde{V}_k\|_2 = \sqrt{2} \|(I - \tilde{S}_k)^{-1} \tilde{S}_k\|_F \leq \frac{4}{3} (2m)^{1/2} \hat{\gamma}_n \tilde{\kappa}_F(B)$$

where

$$\hat{\gamma}_n = \frac{\tilde{c}_n \varepsilon}{1 - \tilde{c}_n \varepsilon}, \quad \tilde{\kappa}_F(B) = \min_{\text{diag } D > 0} \|AD\|_F / \sigma_{\min}(AD)$$

The matrix D is defined in [1] to be *any* positive definite diagonal matrix. Therefore, it follows that

$$\|\tilde{U}_k\|_F = \|\tilde{L}_k^T\|_F \leq \mathcal{O}(\varepsilon) \tilde{\kappa}_F(B), \quad \|\tilde{L}_k\|_F^p \leq \mathcal{O}(\varepsilon^p) \tilde{\kappa}_F^p(B)$$

and thus the matrix inverse from the Neumann series is given by

$$\begin{aligned} T_k &= (I + \tilde{L}_k)^{-1} = I - \tilde{L}_k + \tilde{L}_k^2 - \tilde{L}_k^3 + \dots \\ &= I - \tilde{L}_k + \mathcal{O}(\varepsilon^2) \kappa^2(B) \end{aligned}$$

The growth of the condition number above is related to the norm-wise relative backward error

$$\beta(\mathbf{x}^{(k)}) = \frac{\|\mathbf{r}^{(k)}\|_2}{\|\mathbf{b}\|_2 + \|A\|_\infty \|\mathbf{x}^{(k)}\|_2}$$

and in particular, $\beta(\mathbf{x}^{(k)}) \kappa([\mathbf{r}^{(0)}, AV_k]) = \mathcal{O}(1)$

4. Low-synchronization MGS-GMRES. The MGS–GMRES orthogonalization algorithm is the QR factorization of a matrix B formed by adding a new column to V_k in each iteration

$$[\mathbf{r}^{(0)}, AV_m] = V_{m+1} [\|\mathbf{r}^{(0)}\| \mathbf{e}_1, H_{m+1,m}].$$

We remind the reader that bold-face with superscripts (e.g., $\mathbf{r}^{(0)}$) denote the residual in the GMRES algorithm and subscripting (e.g., $r_{1:i+1,i+2}$) denotes the corresponding element in the upper triangular matrix R .

The MGS-GMRES algorithm was proven to be backward stable for the solution of linear systems $A\mathbf{x} = \mathbf{b}$ in [1] and orthogonality is maintained to $\mathcal{O}(\varepsilon) \kappa(B)$, depending upon the condition number of the matrix $B = \kappa([\mathbf{r}^{(0)}, AV_k])$. The normalization of the Krylov vector \mathbf{v}_{i+1} at iteration $i+1$ represents the delayed scaling of the vector \mathbf{v}_{i+2} in the matrix-vector product $\mathbf{v}_{i+2} = A\mathbf{v}_{i+1}$. Therefore, an additional Step 8 is required in the one-reduce Algorithm 4.1, $r_{1:i+1,i+2} = r_{1:i+1,i+2}/r_{i+1,i+1}$ and $\mathbf{v}_{i+1} = \mathbf{v}_{i+1}/r_{i+1,i+1}$. The diagonal element of the R matrix, corresponds to $H_{i+1,i}$, in the Arnoldi QR factorization of the matrix B , and is updated after the MGS projection in Step 12 of the GMRES Algorithm 4.1. The higher computational speed on a GPU is achieved when the correction matrix is replaced by $T_{i+1} = (I - L_{i+1})$ in Step 11 of the GMRES Algorithm 4.1, resulting in a matrix-vector multiply

The most common convergence criterion when solving linear systems of the form $A\mathbf{x} = \mathbf{b}$ in existing iterative solver frameworks is based upon the relative residual,

$$(4.1) \quad \frac{\|\mathbf{r}^{(k)}\|_2}{\|\mathbf{b}\|_2} = \frac{\|\mathbf{b} - A\mathbf{x}^{(k)}\|_2}{\|\mathbf{b}\|_2} < tol,$$

where tol is some user-defined convergence tolerance. However, when the columns of V_k become linearly dependent, as indicated by $\|S_k\|_2 = 1$, the orthogonality of the Krylov vectors is completely lost. Then the convergence of MGS-GMRES flattens or stalls at this iteration. Due to the relationship with the backward error for solving linear systems $A\mathbf{x} = \mathbf{b}$, elucidated by Prager and Oettli [15] and Rigal and Gaches [16], the backward stability analysis of Paige et al. [1] relies instead upon the norm-wise relative backward error (NRBE) reaching machine precision.

Algorithm 4.1 Truncated Neumann Series MGS-GMRES

Input: Matrix A ; right-hand side vector \mathbf{b} ; initial guess vector $\mathbf{x}^{(0)}$

Output: Solution vector \mathbf{x}

```

1:  $\mathbf{r}^{(0)} = \mathbf{b} - A\mathbf{x}^{(0)}$ ,  $\mathbf{v}_1 = \mathbf{r}^{(0)}$ .
2:  $\mathbf{v}_2 = A\mathbf{v}_1$ 
3:  $(V_2, R, L_2) = \text{mgs}(V_2, R, L_1)$ 
4: for  $i = 1, 2, \dots, m$  do
5:    $\mathbf{v}_{i+2} = A\mathbf{v}_{i+1}$  ▷ Matrix-vector product
6:    $[L_{:,i+1}^T, \mathbf{r}_{i+2}] = V_{i+1}^T[\mathbf{v}_{i+1}, \mathbf{v}_{i+2}]$  ▷ Global synchronization
7:    $r_{i+1,i+1} = \|\mathbf{v}_{i+1}\|_2$ 
8:    $\mathbf{v}_{i+1} = \mathbf{v}_{i+1}/r_{i+1,i+1}$  ▷ Lagged normalization
9:    $r_{1:i+1,i+2} = r_{1:i+1,i+2}/r_{i+1,i+1}$  ▷ Scale for Arnoldi
10:   $L_{:,i+1}^T = L_{:,i+1}^T/r_{i+1,i+1}$ 
11:   $r_{1:i+1,i+2} = T_{i+1} r_{1:i+1,i+2}$  ▷ Projection Step
12:   $\mathbf{v}_{i+2} = \mathbf{v}_{i+2} - V_{i+1} r_{1:i+1,i+2}$ 
13:   $H_i = \mathbf{r}_{i+1}$ 
14:   Apply Givens rotations to  $H_i$ 
15: end for
16:  $\mathbf{y}_m = \text{argmin}(\|H_m \mathbf{y}_m - \|\mathbf{r}_0\|_2 \mathbf{e}_1\|)_2$ 
17:  $\mathbf{x} = \mathbf{x}^{(0)} + V_m \mathbf{y}_m$ 

```

5. Algebraic Multigrid Preconditioner. Neumann series also naturally arise when employing certain smoothers in AMG, and in particular, polynomial Gauss-Seidel and ILU smoothers. Before analyzing this, necessary background information on AMG is first provided.

AMG [5] is an effective method for solving linear systems of equations. In theory, AMG can solve a linear system with n unknowns in $\mathcal{O}(n)$ operations, and even though it was originally developed as a solver, it is now common practice to use AMG as a preconditioner to a Krylov method; in particular, when such Krylov solvers are applied to large-scale linear systems arising in physics-based simulations. As either a solver or preconditioner, an AMG method accelerates the solution of a linear system $A\mathbf{x} = \mathbf{b}$ through error reduction by using a sequence of coarser matrices called a *hierarchy*. These matrices will be denoted A_k , where $k = 0 \dots m$, and $A_0 = A$. Each A_k has dimensions $m_k \times m_k$ where $m_k > m_{k+1}$ for $k < m$. For the purposes of this paper, assume that

$$(5.1) \quad A_k = R_k A_{k-1} P_k,$$

for $k > 0$, where P_k is a rectangular matrix with dimensions $m_{k-1} \times m_k$. P_k is referred to as a *prolongation matrix* or *prolongator*. R_k is the *restriction matrix* and $R_k = P_k^T$ in the Galerkin formulation of AMG. Associated with each A_k , $k < m$, is a solver called a *smoother*, which is usually a stationary iterative method, e.g. Gauss-Seidel, polynomial, or incomplete factorization. The *coarse solver* used for A_m (the lowest level in the hierarchy) is often a direct solver, although it may be an iterative method if A_m is singular.

The setup phase of AMG is nontrivial for several reasons. Each prolongator P_k is developed algebraically from A_{k-1} . Once the transfer matrices are determined, the coarse-matrix representations are computed recursively from A through sparse triple-matrix multiplication. This describes a V -cycle, the simplest complete AMG cycle; refer to Algorithm 1 in the recent paper by Thomas et al. [12] for a complete description. AMG methods achieve optimality (constant work per degree of freedom in A_0) through error reductions by the smoother and corrections propagated from coarser levels.

5.1. Ruge–Stüben Classical AMG. We now give an overview of classical Ruge–Stüben AMG, starting with notation. Interpolation is formulated in terms of matrix operations. Point j is a neighbor of i if and only if there is a non-zero element a_{ij} of the matrix A . Point j strongly influences i if and only if

$$(5.2) \quad |a_{ij}| \geq \theta \max_{k \neq i} |a_{ik}|,$$

where θ is the strength of connection threshold, $0 < \theta \leq 1$. This strong influence relation is used to select coarse points. These points are retained in the next coarser level, and the remaining fine points are dropped. Let C_k and F_k be the coarse and fine points selected at level k , and let m_k be the number of grid points at level k ($m_0 = n$). Then, $m_k = |C_k| + |F_k|$, $m_{k+1} = |C_k|$, A_k is a $m_k \times m_k$ matrix, and P_k is an $m_{k-1} \times m_k$ matrix. Here, the coarsening is performed row-wise by interpolating between coarse and fine points. The coarsening generally attempts to fulfill two contradictory criteria. In order to ensure that a chosen interpolation scheme is well-defined and of good quality, some close neighborhood of each fine point must contain a sufficient amount of coarse points to interpolate from. Hence the set of coarse points must be rich enough. However, the set of coarse points should be sufficiently small in order to achieve a reasonable coarsening rate. The interpolation should lead to a reduction of roughly five times the number of non-zeros nnz at each level of the V -cycle.

During the setup phase of AMG methods, the multi-level V -cycle hierarchy is constructed consisting of linear systems having exponentially decreasing sizes on coarser levels. A strength-of-connection matrix S , is typically first computed to indicate directions of algebraic smoothness and applied in the coarsening algorithms. The construction of S may be performed efficiently, because each row is computed independently by selecting entries in the corresponding row of A with a prescribed threshold value θ . `hypr-BoomerAMG` provides the parallel maximal independent set (PMIS) coarsening [17], which is modified from Luby's algorithm [18] for finding maximal independent sets using random numbers.

Interpolation operators in AMG transfer residual errors between adjacent levels. There are a variety of interpolation schemes available. Direct interpolation [19] is straightforward to implement in parallel because the interpolatory set of a fine point i is just a subset of the neighbors of i , and thus the interpolation weights can be determined solely by the i -th equation. A bootstrap AMG (BAMG) [20] variant of direct interpolation is generally found to be better than the original formula. The weights w_{ij} are computed by solving the local optimization problem

$$\min \|a_{ii}\mathbf{w}_i^T + a_{i,C_i^s}\|_2 \quad \text{s.t.} \quad \mathbf{w}_i^T \mathbf{f}_{C_i^s} = \mathbf{f}_i,$$

where \mathbf{w}_i is a vector that contains w_{ij} , C_i^s and denotes strong C-neighbors of i and \mathbf{f} is a target vector that needs to be interpolated exactly. For elliptic problems where the near null-space is spanned by constant vectors, i.e., $\mathbf{f} = \mathbf{1}$, the closed-form solution of (5.1) is given by

$$(5.3) \quad w_{ij} = -\frac{a_{ij} + \beta_i/n_{C_i^s}}{a_{ii} + \sum_{k \in N_i^w} a_{ik}}, \quad \beta_i = \sum_{k \in \{\mathbf{f}_i \cup C_i^w\}} a_{ik},$$

where $n_{C_i^s}$ denotes the number of points in C_i^s , C_i^w the weak C-neighbors of i , \mathbf{f}_i the F-neighbors, and N_i^w the weak neighbors. A known issue of PMIS coarsening is that it can result in F-points without C-neighbors [21]. In such situations, distance-one interpolation algorithms often work well, whereas interpolation operators that can reach C-points at a larger range, such as the extended interpolation [21], can generally yield much better convergence. However, implementing extended interpolation is more complicated because the sparsity pattern of the interpolation operator cannot be determined a priori, which requires dynamically combining C-points in a distance-2 neighborhood. With minor modifications to the original form, it turns out that the extended interpolation operator can be rewritten by using standard sparse matrix computations such as matrix-matrix (M-M) multiplication and diagonal scaling with certain FF - and FC -sub-matrices. The coarse-fine C-F splitting of the coarse matrix A is given by

$$A = \begin{bmatrix} A_{FF} & A_{FC} \\ A_{CF} & A_{CC} \end{bmatrix}$$

where A is assumed to be decomposed into $A = D + A^s + A^w$, the diagonal, the strong part and weak part respectively, and A_{FF}^w , A_{FC}^w , A_{FF}^s and A_{FC}^s are the corresponding sub-matrices of A^w and A^s .

The full prolongation operator is given by

$$P = \begin{bmatrix} W \\ I \end{bmatrix}$$

The extended "MM-ext" interpolation now takes the form

$$W = -[(D_{FF} + D_\gamma)^{-1}(A_{FF}^s + D_\beta)] [D_\beta^{-1} A_{FC}^s]$$

with

$$D_\beta = \text{diag}(A_{FC}^s \mathbf{1}_C) \quad D_\gamma = \text{diag}(A_{FF}^w \mathbf{1}_F + A_{FC}^w \mathbf{1}_C),$$

This formulation allows simple and efficient implementations. Similar approaches that are referred to as “MM-ext+i” modified from the original extended+i algorithm [21] and “MM-ext+e” are also available in BoomerAMG. See [22] for details on the class of M-M based interpolation operators.

Aggressive coarsening reduces the grid and operator complexities of the AMG hierarchy, where a second coarsening is applied to the C-points obtained from the first coarsening to produce a smaller set of final C-points. The A-1 aggressive coarsening strategy described in [19] is employed in our studies. The second PMIS coarsening is performed with the CC block of $S^{(A)} = S^2 + S$ that has nonzero entry $S_{ij}^{(A)}$ if i is connected to j with at least a path of length less than or equal to two. Aggressive coarsening is usually used with polynomial interpolation [23] which computes a second-stage interpolation matrix P_2 and combined with the first-stage P_1 as $P = P_1 P_2$. The aforementioned MM-based interpolation is also available for the second stage. Finally, Galerkin triple-matrix products are used to build coarse-level matrices $A_c = P^T A P$ involving the prolongation P and restriction P^T operators. Falgout et al. [24] provides the additional details omitted here on the algorithms employed in hypre for computing distributed and parallel sparse matrix-matrix M–M multiplications.

5.2. Polynomial Gauss–Seidel Smoother. To solve a linear system $A\mathbf{x} = \mathbf{b}$, the Gauss-Seidel (GS) iteration is based upon the matrix splitting $A = L + D + U$, where L and U are the strictly lower and upper triangular parts of the matrix A , respectively. Then, the traditional GS updates the solution based on the following recurrence,

$$(5.4) \quad \mathbf{x}^{(k+1)} := \mathbf{x}^{(k)} + M^{-1} \mathbf{r}^{(k)}, \quad k = 0, 1, 2, \dots$$

where $\mathbf{r}^{(k)} = \mathbf{b} - A\mathbf{x}^{(k)}$, $A = M - N$, and $M = L + D$, $N = -U$ or $M = U + D$, $N = -L$ for the forward or backward sweeps, respectively. In the following, $\mathbf{x}^{(k)}$ is the k -th Gauss-Seidel iterate. To avoid explicitly forming the matrix inverse M^{-1} in (5.4), a sparse-triangular solve is used to apply M^{-1} to the current residual vector $\mathbf{r}^{(k)}$.

To improve the parallel scalability, hypre implements a hybrid variant of GS [25], where the neighboring processes first exchange the elements of the solution vector on the boundary of the subdomain assigned to an a parallel process (MPI rank), but then each MPI rank independently applies the local relaxation. Furthermore, in hypre, each rank may apply multiple local GS sweeps for each round of the neighborhood communication. With this approach, each local relaxation updates only the local part of the vector $\mathbf{x}^{(k+1)}$ (during the local relaxation, the non-local solution elements on the boundary are not kept consistent among the neighboring ranks). This hybrid algorithm is shown to be effective for many problems [25].

A polynomial GS relaxation employs a fixed number of “inner” stationary iterations for approximately solving the triangular system with M ,

$$(5.5) \quad \widehat{\mathbf{x}}^{(k+1)} := \widehat{\mathbf{x}}^{(k)} + \widehat{M}^{-1}(\mathbf{b} - A\widehat{\mathbf{x}}^{(k)}), \quad k = 0, 1, 2, \dots$$

where \widehat{M}^{-1} represents the approximate triangular system solution, i.e., $\widehat{M}^{-1} \approx M^{-1}$. A Jacobi inner iteration is employed to replace the direct triangular solve. In particular, if $\mathbf{g}_k^{(j)}$ denotes the approximate solution from the j -th inner iteration at the k -th outer GS iteration, then the initial solution is chosen to be the diagonally scaled residual vector,

$$(5.6) \quad \mathbf{g}_k^{(0)} = D^{-1} \mathbf{r}^{(k)},$$

and the $(j + 1)$ -st Jacobi iteration computes the approximate solution by the recurrence

$$(5.7) \quad \mathbf{g}_k^{(j+1)} := \mathbf{g}_k^{(j)} + D^{-1}(\mathbf{r}^{(k)} - (L + D)\mathbf{g}_k^{(j)})$$

$$(5.8) \quad = D^{-1}(\mathbf{r}^{(k)} - L\mathbf{g}_k^{(j)}).$$

When “zero” inner sweeps are performed, the polynomial GS recurrence becomes

$$\widehat{\mathbf{x}}^{(k+1)} := \widehat{\mathbf{x}}^{(k)} + \mathbf{g}_k^{(0)} = \widehat{\mathbf{x}}^{(k)} + D^{-1}(\mathbf{b} - A\widehat{\mathbf{x}}^{(k)}),$$

and this special case corresponds to Jacobi iteration for the global system, or local system on each MPI rank. When p inner iterations are performed, it follows that

$$\begin{aligned}\widehat{\mathbf{x}}^{(k+1)} &:= \widehat{\mathbf{x}}^{(k)} + \text{vect}g_k^{(p)} = \widehat{\mathbf{x}}^{(k)} + \sum_{j=0}^p (-D^{-1}L)^j D^{-1}\widehat{\mathbf{r}}^{(k)} \\ &\approx \widehat{\mathbf{x}}^{(k)} + (I + D^{-1}L)^{-1} D^{-1}\widehat{\mathbf{r}}^{(k)} = \widehat{\mathbf{x}}^{(k)} + M^{-1}\widehat{\mathbf{r}}^{(k)},\end{aligned}$$

where M^{-1} is approximated by the degree- p Neumann expansion and $\widehat{\mathbf{r}}^{(k)}$ is the residual following the iterated inner solve (e.g., $\widehat{\mathbf{r}}^{(k)} = \mathbf{b} - A\widehat{\mathbf{x}}^{(k)}$). Note that $D^{-1}L$ is strictly lower triangular and nilpotent so that the Neumann series converges in a finite number of steps.

5.3. ILU Smoothers with Scaled Factors and Iterated Triangular Solves. When applying an incomplete LU factorization as the smoother, careful consideration of algorithms which solve the triangular systems is needed. A direct triangular solver is comparatively more expensive on a GPU than iterations using sparse matrix vector products, and thus Jacobi iteration was proposed in [13]. However, in cases when the triangular factors are highly non-normal, the Jacobi iterations may diverge [13, 26, 27]. Note that triangular matrices are necessarily non-normal [28], and three methods to mitigate the degree of non-normality are explored: (1) The incomplete LDU factorization with row scaling, (2) reordering to enforce symmetric sparsity patterns, and (3) row and column scaling. For (2), several reordering strategies are considered, and for (3), the Ruiz strategy [29] is considered. Before discussing both experimental and theoretical analyses for these approaches, some background on (non)-normality is first provided.

5.3.1. Jacobi Iteration and Normality. The Jacobi iteration for solving $Ax = b$ can be written in the compact form below, with the regular splitting $A = M - N$, $M = D$ and $N = D - A$. The iteration matrix G is defined as $G = I - D^{-1}A$ and

$$(5.9) \quad \mathbf{x}^{(k+1)} = G \mathbf{x}^{(k)} + D^{-1}\mathbf{b}$$

or in the non-compact form, with $M = A - D$

$$(5.10) \quad \mathbf{x}^{(k+1)} = \mathbf{x}^{(k)} + D^{-1}(\mathbf{b} - A\mathbf{x}^{(k)})$$

where D is the diagonal part of A . For the triangular systems resulting from the ILU factorization $A \approx LU$ (as opposed to the splitting $A = D + L + U$), we denote the iteration matrices as G_L and G_U for the lower and upper triangular factors, L and U respectively. Let D_L and D_U be the diagonal parts of the triangular factors L and U and I denotes the identity matrix. Assume L has a unit diagonal, then

$$(5.11) \quad G_L = D_L^{-1}(D_L - L) = I - L$$

$$(5.12) \quad G_U = D_U^{-1}(D_U - U) = I - D_U^{-1}U$$

A sufficient condition for the Jacobi iteration to converge is that the spectral radius of the iteration matrix is less than unity, or $\rho(G) < 1$. G_L is strictly lower and G_U is strictly upper triangular, which implies that the spectral radius of both iteration matrices is zero. Therefore, the Jacobi iteration converges in the asymptotic sense for any triangular system. However, the convergence of the Jacobi method may be affected by the degree of non-normality of the matrix, which is now defined.

A normal matrix $A \in \mathbb{C}^{n \times n}$ satisfies $A^*A = AA^*$, and so a matrix that is non-normal can be defined in terms of the difference between A^*A and AA^* to indicate the degree of non-normality. Measures of nonnormality and the behavior of nonnormal matrices, have been extensively considered; see [14, 30–32]. In this paper, we use Henrici’s definition of the departure from normality of a matrix $A \in \mathbb{C}^{n \times n}$

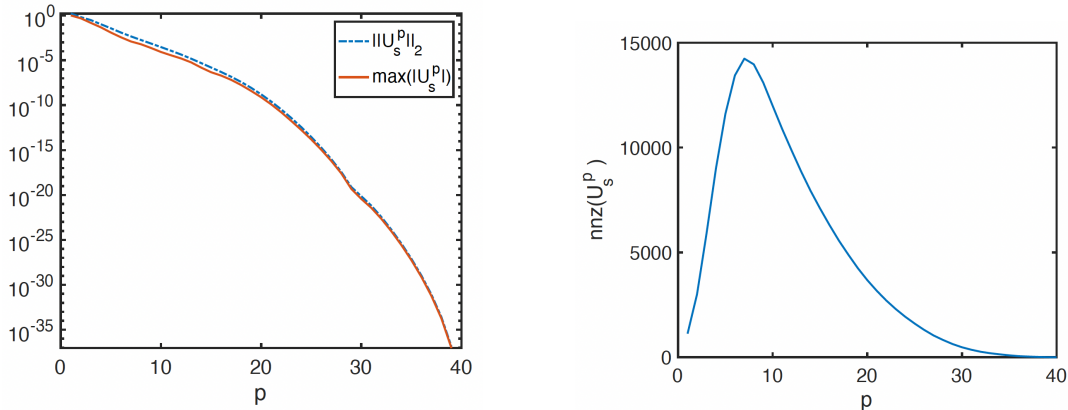
$$(5.13) \quad \text{dep}(A) = \sqrt{\|A\|_F^2 - \|D\|_F^2},$$

where $D \in \mathbb{C}^{n \times n}$ is the diagonal matrix containing the eigenvalues of A [14]. By no means is this the only practical metric for describing the degree of nonnormality, however, it is particularly useful in the context of the current paper.

5.3.2. Iterating with an LDU Factorization. Given an incomplete LU factorization, when either factoring out the D matrix from the incomplete LU , or computing an incomplete LDU factorization, the iteration matrix (5.12) simplifies to $G = U_s$, where U_s is a strictly upper triangular matrix (SUT). In particular, this leads naturally to a Neumann series, where for $\mathbf{f} = D_U^{-1}\mathbf{b}$

$$\begin{aligned}
 \mathbf{x}^{(k+1)} &= \mathbf{f} - U_s \mathbf{f} + U_s^2 \mathbf{f} - \dots + (-1)^k U_s^k \mathbf{f} \\
 (5.14) \quad &= (I - U_s + U_s^2 - \dots + (-1)^k U_s^k) \mathbf{f} \\
 &= (I - U_s)^{-1} \mathbf{f}.
 \end{aligned}$$

In [12], an extensive empirical analysis shows that for certain drop tolerances, and amounts of fill, $\|U_s\|_2 < 1$. Thus, the convergence of the Neumann series is guaranteed. Even for those drop tolerances where $\|U_s\|_2 < 1$ does not hold, $\|U_s^p\|_2 < 1$ for moderate p , and further $\|U_s^p\|_2$ goes to 0 fairly quickly. Furthermore, for the (scaled) matrices considered in the current paper, a correlation exists between the maximum value (in magnitude) of U_s^p and this rate of convergence. Figure 1a, compares $\max |(U_s^p)_{ij}|$ and $\|U_s^p\|_2$ for increasing values of p for a PeleLM matrix dimension $N = 331$ when computing an incomplete LDU factorization. While the number of nonzeros in U_s^p increases for $p \leq 6$, the norm rapidly decreases, and $nnz(U_s^p) = 0$ by $p = 39$; see Figure 1b. Of course, for strictly upper triangular matrices, U_s^p is guaranteed to be the zero matrix when $p = n$, however, numerical nilpotence occurs much sooner (i.e., $p \ll n$). Building a theoretical framework to describe the relationship between these metrics is part of our ongoing work, and we refer to [12] for more empirical analyses of $\|U_s^p\|_2$. In particular, a relationship between larger drop tolerances and smaller fill-in when computing the ILU factorizations is observed when using row scaling.



(a) $\max |(U_s^p)_{ij}|$ and $\|U_s^p\|_2$ for $p = 1 : 39$. For $p \geq 40$, both $\max |(U_s^p)_{ij}|$ and $\|U_s^p\|_2$ are zero.

(b) Number of nonzeros in U_s^p for $p = 1 : 39$. For $p \geq 40$, $nnz(U_s^p) = 0$.

Fig. 1: Comparison of $\max |(U_s^p)_{ij}|$, $\|U_s^p\|_2$, and $nnz(U_s^p)$ for a linear system from PeleLM of dimension $N = 331$.

5.3.3. Matrix Re-Orderings and Non-Normality. Richardson iteration can be interpreted in a nonlinear sense as a continuous in space and discrete time scheme for a heat-equation that is integrated to steady state. The Jacobi iteration can also be considered as a time integrator and the tools of nonlinear stability analysis can be applied. In particular, the recent work of Asllani et al. [33] establishes the connection between non-normality, pseudo-spectra and the asymptotic convergence behaviour of such nonlinear schemes.

For the purposes of iteratively solving triangular systems, one might reasonably presuppose that matrix re-orderings have an effect on the departure from normality of the L and U factors. In particular,

re-ordering can minimize the amount of fill-in and thereby reduce the $dep(L)$ and $dep(U)$. Furthermore, symmetric sparsity patterns of the factors would lead to a similar number of Jacobi iterations for the triangular solves. Indeed, this is observed empirically and in the case of non-symmetric matrices, the structural symmetry resulting from the approximate minimum degree (AMD) re-ordering in combination with a row-scaled LDU factorization leads to a small departure from normality and a rapidly converging Jacobi iteration.

Consider the Nalu-Wind pressure continuity equation matrix A of dimension $N = 3.2$ Million. Several different matrix re-orderings are applied to A , followed by an incomplete LDU factorization. Then the Jacobi iteration is applied to the approximate linear system $LDUx = b$ where the right-hand side b is obtained from the extracted pressure system. The relative residual for each of the triangular solves is reported in Table 1. The matrix re-orderings consisted of the symmetric reverse Cuthill-McKee ('symrcm') [34], approximate minimum degree or AMD ('amd') [35], symmetric AMD ('symamd'), and nested dissection ('dissect') [36] in Matlab combined with an ILU(0) factorization and five (5) Jacobi iterations for the systems $Ly = b$ and $Ux = y$.

	symrcm	amd	symamd	dissect
$\ b - L y_k\ _2 / \ b\ _2$	0.33	4.2e-5	1.8e-5	8.4e-4
$\ y - U v_k\ _2 / \ y\ _2$	15.4	8.1e-5	4.1e-5	8.70e-3

Table 1: Relative residuals for $LDUx = b$ from ILU(0) factorization after five (5) Jacobi iterations to solve L and U systems for a linear system from Nalu-Wind model with dimension $N = 3.2$ million.

Clearly, the AMD re-orderings lead to the lowest relative residuals and thus are candidates to be evaluated for a GMRES+AMG solver for the slightly non-symmetric Nalu-Wind pressure systems. Table 2 displays the departure from normality $dep(U)$ and $dep(L)$ after re-ordering the coefficient matrix followed by row scaling using the ILU(0) factorization and row scaled LDU .

	unscaled	symrcm	amd	symamd	dissect
$dep(L)$	2.10e+4	1.40e+3	1.06e+3	927.3	1.34e+3
$dep(U)$	2.01e+4	1.05e+3	787.3	782.4	796.5

Table 2: Henrici departure from normality $dep(U)$ for ILU(0) factorization with row scaling LDU for matrices from Nalu-Wind model with dimension $N = 3.2$ million.

The departure from normality without re-ordering or scaling is $dep(U) = 2.1e+4$. There is a clear correlation between the $dep(U)$ for each of the orderings in Table 2 and the size of the relative residuals in Table 1. Thus, a lower value for Henrici's departure from normality is a good predictor of the rapid convergence of the iterative triangular solves.

5.3.4. Iterating with an LU Factorization using Ruiz Scaling. Next, consider the application of the Ruiz strategy [29] directly to the problematic L and U factors themselves. In cases where only an LU factorization is available, this strategy is appealing. The objective is to reduce the condition number of an ill-conditioned matrix, and it is also shown here to be effective in reducing $dep(U)$. A rigorous experimental analysis of this method is given in [12] and in the present paper these results are augmented with theoretical bounds.

The Ruiz algorithm is an iterative procedure that uses row and column scaling such that the resulting diagonal entries of the matrix are one, and all other elements are less than (or equal to) one [29]. Algorithm 5.1 describes the ILUT smoother employing the scaling for non-normal triangular factors, and the practical implementation of this approach is described in more detail in [12].⁴ It is provided here for ease of reference. In Section 6 and for the applications considered in this paper, only the U factor is scaled. However, this algorithm may also be extended to scale the L factor in cases when both L and U are highly non-normal.

⁴Note that row scaling can be used in place of Ruiz scaling by instead constructing $D = \text{diag}(U)$, and letting $\tilde{U} = D^{-1}U$.

Algorithm 5.1 ILUT+Jacobi smoother for C-AMG with Ruiz scaling for non-normal upper triangular factors.

Given $A \in \mathbb{C}^{n \times n}$, $\mathbf{b} \in \mathbb{C}^n$
 Define *droptol* and *lfill*
 Compute $A \approx LU$ with *droptol* and *lfill* imposed
 Define m_L and m_u , total number of Jacobi iterations for solving L and U
 Define $\mathbf{y}^{(0)} = 0$, $\mathbf{v}^{(0)} = \mathbf{y}^{(0)}$
 //Jacobi iteration to approximately solve $L\mathbf{y} = \mathbf{b}$
for $k = 1 : m_L$ **do**
 $\mathbf{y}^{(k)} = \mathbf{y}^{(k-1)} + (\mathbf{b} - L\mathbf{y}^{(k-1)})$
end for
 Apply the Ruiz strategy for U and \mathbf{y} to obtain scaled $\tilde{U} = D_r U D_c$ and $\tilde{\mathbf{y}} = D_r^{-1} \mathbf{y}^{(m_L)}$
 Let $D_u = \text{diag}(\tilde{U})$
 Define $D = D_u^{-1}$
 //Jacobi iteration to approximately solve $\tilde{U}\mathbf{v} = \tilde{\mathbf{y}}$
for $k = 1 : m_U$ **do**
 $\mathbf{v}^{(k)} = \mathbf{v}^{(k-1)} + D(\tilde{\mathbf{y}} - \tilde{U}\mathbf{v}^{(k-1)})$
end for
 //Unscale the approximate solution
 $\mathbf{v} = D_c^{-1} \mathbf{v}^{(m_U)}$

The row and column scaling algorithm results in a transformed linear system $Ax = b$ that now takes the form

$$L D_r U D_c \mathbf{x} = \mathbf{b}$$

and the Jacobi iterations are applied to the upper triangular matrix $D_r U D_c$. Here, D_r and D_c represent row and column scaling, respectively, of the U factor. However, this matrix has a unit diagonal and the iterations can be expressed in terms of a Neumann series. When an LDU or LDL^T factorization is available, the series can be directly obtained from U or L^T as these are strictly upper triangular matrices. The D matrix can also be extracted from either of these matrices by row scaling when possible.

When applying scaling to U , a matrix $U = I + U_s$ results, with I the identity matrix of dimension n , and U_s strictly upper triangular. Thus, the inverse of such a matrix can be expressed as a Neumann series

$$(5.15) \quad (I + U_s)^{-1} = I - U_s + U_s^2 - \dots$$

Because U_s is upper triangular and nilpotent, the above sum is finite, and the series is also guaranteed to converge when $\|U_s\|_2 < 1$.

A loose upper bound for $\|U_s\|_2$ can be derived and attributed in part to the fill level permitted in the ILU factorization.

THEOREM 5.1. *Let p represent the number of nonzero elements permitted in the L and U factors of an incomplete LU factorization. Then for scaled $U \in \mathbb{C}^{n \times n}$ such that $U = I + U_s$, with I the identity matrix, and U_s a strictly upper triangular matrix,*

$$(5.16) \quad \|U_s\|_2 \leq \|U_s\|_F \leq \sqrt{n(p-1)}.$$

Proof. The proof follows from taking the Frobenius norm of a strictly upper triangular matrix with a maximum of $p-1$ nonzero elements per row, and the observation that $u_{ij} \leq 1$ for all i, j . \square

The bound in Theorem 5.1 is obviously pessimistic, even when allowing only a small fill level in the ILU factorization. However, it is observed in practice that after scaling, $\|U_s\|_2 < 1$, and this is often true for the ILUT smoothers with *fill* ≤ 20 for the applications considered in this paper. An increase in the size of $\|U_s\|_2$ is observed as the level of fill increases; see Table 3 for a comparison of $\|U_s\|_2$ with $\|U_s\|_F$ and the theoretical bound in Theorem 5.1, when varying the fill level.

	$fill = 5$	$fill = 10$	$fill = 20$	$fill = 50$	$fill = 200$
$\ U_s\ _2$	0.679	0.753	0.87	1.04	1.22
$\ U_s\ _F$	120.69	121.86	122.22	122.39	122.44
Theorem 5.1 Bound	283.21	357.32	519.17	833.74	1.68e+3

Table 3: Comparison of $\|U_s\|_2$, $\|U_s\|_F$, and the theoretical bound provided in Theorem 5.1 for different amounts of fill permitted in the ILU factorization, and after applying scaling for a linear system from PeleLM of dimension $N = 14186$.

The results in Table 3 indicate not only that the bound given in Theorem 5.1 is less pessimistic for $\|U_s\|_F$, but also (and more importantly) that it may be reasonably conjectured that for small levels of fill, $\|U_s\|_2 < 1 < \|U_s\|_F$. In this case, both a lower and upper bound on $\|U_s\|_2$ may be derived as follows.

THEOREM 5.2. *Let U_s be defined as in Theorem 5.1 and $r = \text{rank}(U_s)$. If $\|U_s\|_2 < 1 < \|U_s\|_F$, then $\|U_s\|_2$ is bounded as*

$$(5.17) \quad \frac{1}{\sqrt{r}} \leq \|U_s\|_2 < 1.$$

Proof. The proof follows from the fact that $\|U_s\|_2 \leq \|U_s\|_F \leq \sqrt{r}\|U_s\|_2$. \square

The rank of U_s may also provide insight into the relationship between $\|U_s\|_2$ and the convergence behavior of the iterative method. In particular, it was found that for the PeleLM matrix dimension $N = 14186$, and $droptol = 1e-1$ and $fill = 5$ for the ILUT factorization, $\text{rank}(U_s) \approx 3500$. Whether or not the low-rank nature of U_s can be exploited is a question for future investigation. For now, consider the largest singular values and the convergence rate of the Krylov method. $\|U_s\|_2$ is also equal to the largest singular value of U_s , denoted as $\sigma_1(U_s)$. The magnitude of $\sigma_1(U_s)$ is clearly related to convergence rate of the iterative method. In particular, when $\|U_s\|_2 = \sigma_1(U_s) > 1$ (e.g., when $fill > 20$ for the system considered here), faster convergence is achieved compared with when $\|U_s\|_2 = \sigma_1(U_s) < 1$ (e.g., when $fill \leq 20$); see Table 4 for a comparison of the iterations required to reduce the relative residual below $1e-5$ with $\sigma_1(U_s)$ when varying the fill. When the fill increases, $\sigma_1(U_s)$ grows larger, and the number of iterations decreases. This is especially interesting because the Neumann series in (5.15) converges for $\|U_s\|_2 < 1$, and yet the fastest GMRES convergence is observed for $\|U_s\|_2 > 1$ for this particular application. Ongoing work seeks to build a theoretical framework to describe this relationship. Note here that the ILUT smoother is applied on all levels of the V -cycle, whereas in later results a hybrid approach is employed where the ILUT smoother is applied only at the finest level.

	$fill = 5$	$fill = 10$	$fill = 20$	$fill = 50$	$fill = 200$
$\sigma_1(U_s)$	0.679	0.753	0.87	1.04	1.22
GMRES Iters	7	6	3	2	2

Table 4: Comparing the largest singular value of U_s with GMRES iteration counts for different fill levels permitted in the ILU factorization for a linear system from PeleLM of dimension $N = 14186$.

Next, an upper bound on the $\text{dep}(U)$ is derived after scaling is applied, noting that an analogous statement can be made for $\text{dep}(L)$.

THEOREM 5.3. *Let $U \in \mathbb{C}^{n \times n}$ be a scaled upper triangular matrix such that $U = I + U_s$, with I the identity matrix of dimension n and U_s a strictly upper triangular matrix with elements $u_{i,j} \leq 1$. For $\nu = \|U_s\|_F$*

$$(5.18) \quad \text{dep}(U) \leq \sqrt{(2\sqrt{n} + \nu)\nu}.$$

Proof. For this proof, the Frobenius norm subscript is dropped for simplicity. With $U = I + U_s$, it follows that

$$\begin{aligned}
 (5.19) \quad \text{dep}(U)^2 &= \|U\|^2 - \|D\|^2 = \|I + U_s\|^2 - n \\
 (5.20) \quad &= \|I + U_s\| \|I + U_s\| - n \leq (\sqrt{n} + \|U_s\|)^2 - n \\
 (5.21) \quad &= (2\sqrt{n} + \|U_s\|) \|U_s\|.
 \end{aligned}$$

Denoting $\nu = \|U_s\|_F$ and taking the square root of (5.21), the desired result is obtained. \square

Theorem 5.3 is completely independent of $\kappa_2(U)$ and gives a practical bound on the departure from normality of a scaled U . Consider for example $n = 10^9$ and $\|U_s\| = 0.8$; Theorem 5.3 guarantees that after scaling, $\text{dep}(U)$ can be no larger than 225. In general, even if $\|U_s\|_F$ is larger than one, as long as it is modest (e.g. $O(10)$ or even $O(10^2)$), a reasonable bound on $\text{dep}(U)$ is obtained after scaling the upper triangular factor.

	<i>fill</i> = 5	<i>fill</i> = 10	<i>fill</i> = 20	<i>fill</i> = 50	<i>fill</i> = 200
$\text{dep}(U)$ before	7.98e+7	1.06e+8	1.12e+8	1.16e+8	1.17e+8
$\text{dep}(U)$ after	19.47	25.79	27.42	28.16	28.40
Theorem 5.3 Bound	208.12	209.48	209.89	210.08	210.14

Table 5: $\text{dep}(U)$ before and after Ruiz scaling, and the theoretical bound provided in Theorem 5.3, for different fill levels permitted in the ILU factorization. $N = 14186$.

Theorem 5.3 may also provide a relatively inexpensive test for early termination of the Ruiz algorithm. In practice, the algorithm generally takes a maximum of five iterations to converge, but the departure from normality does not necessarily decrease for each iteration. In particular, $\text{dep}(U)$ reaches a minimum after only the first or second iteration, with a slight increase for the remaining iterations. Thus, if at step k of the Ruiz algorithm, $\text{dep}(U_s) < \text{tol}$ (where tol can be some modest scalar multiple of the bound given in Theorem 5.3), the algorithm can be terminated early. For the systems considered here, this can result in a potential cost savings of up to four iterations of the Ruiz algorithm.

While scaling does not guarantee that the resulting matrix is diagonally dominant, when a large drop tolerance and small fill-in value are specified, the resulting L and U factors are nearly diagonally dominant, which we define as follows. Here, we consider only the U factor, but analogous results can be derived for L .

DEFINITION 5.4. Let u_{ii} be the diagonal elements of $U \in \mathbb{C}^{n \times n}$ for $i = 1, 2, \dots, n$ and $\delta = \max_i \delta_i$, where $\delta_i > 0$ is such that

$$(5.22) \quad |u_{ii}| \geq \sum_{j \neq i} |u_{ij}| - \delta_i$$

for all $i = 1, 2, \dots, n$. U is nearly (row) diagonally dominant if and only if

$$(5.23) \quad |u_{ii}| \geq \sum_{j \neq i} |u_{ij}| - \delta.$$

The following theorem now takes into consideration the near diagonal dominance of U , in cases where U takes the form $U = I + U_s$, as is the case when applying scaling to the U factor of an incomplete LU factorization.

THEOREM 5.5. Assume $U = I + U_s \in \mathbb{C}^{n \times n}$, for U_s strictly upper triangular. If U is nearly diagonally dominant, then

$$(5.24) \quad \text{dep}(U) \leq \sqrt{n}(1 + \delta),$$

where δ is as defined in definition 5.4.

Proof.

$$(5.25) \quad dep(U)^2 = \|U\|^2 - \|D\|^2 = \sum_{i=1}^n \sum_{j=1}^n |u_{ij}|^2 - n$$

$$(5.26) \quad = \sum_{i=1}^n (|u_{ii}|^2 + \sum_{\substack{j=1, \\ j \neq i}}^n |u_{ij}|^2) - n$$

$$(5.27) \quad \leq \sum_{i=1}^n (1 + (1 + \delta)^2) - n$$

$$(5.28) \quad = n(1 + (1 + \delta)^2) - n$$

$$(5.29) \quad = n(1 + \delta)^2.$$

Taking the square root of (5.29) gives the desired result. \square

While this bound is not tighter than the one given in Theorem 5.5, it establishes the connection between the fill level and $dep(U)$. Specifically, when a higher fill is used in the ILU factorization, the resulting triangular factors have the potential to be far from diagonally dominant (resulting from more nonzeros allowed in each row). Theorem 5.3 guarantees that as δ grows smaller (i.e., as U becomes closer to diagonally dominant), the upper bound on $dep(U)$ decreases monotonically.

6. Numerical Results. To study the performance of the iterated Gauss-Seidel and ILU smoothers in a practical setting, incompressible fluid flow simulations were performed with Nalu-Wind and PeleLM. These are two of the primary fluid mechanics codes for the application projects chosen for the DOE Exascale Computing Project (ECP) and used for high-fidelity simulations. We describe both next.

6.1. Nalu-Wind Model. Nalu-Wind solves the incompressible Navier-Stokes equations, with a pressure projection scheme [6]. The governing equations are discretized in time with a BDF-2 integrator, where an outer Picard fixed-point iteration is employed to reduce the nonlinear system residual at each time step. Within each time step, the Nalu-Wind simulation time is often dominated by the time required to setup and solve the linearized governing equations. The pressure systems are solved using MGS-GMRES with an AMG preconditioner, where a polynomial Gauss-Seidel smoother is now applied as described in Mulleney et al. [10]. Hence, Gauss-Seidel is a compute time intensive component, when employed as a smoother within an AMG V -cycle.

The McAlister experiment for wind-turbine blades is an unsteady RANS simulation of a fixed-wing, with a NACA0015 cross section, operating in uniform inflow. Resolving the high-Reynolds number boundary layer over the wing surface requires resolutions of $\mathcal{O}(10^{-5})$ normal to the surface resulting in grid cell aspect ratios of $\mathcal{O}(40,000)$. These high aspect ratios present a significant challenge. Overset meshes were employed [6] to generate body-fitted meshes for the wing and the wind tunnel geometry. The simulations were performed for the wing at 12 degree angle of attack, 1 m chord length, denoted c , 3.3 aspect ratio, i.e., $s = 3.3c$, and square wing tip. The inflow velocity is $u_\infty = 46$ m/s, the density is $\rho_\infty = 1.225$ kg/m³, and dynamic viscosity is $\mu = 3.756 \times 10^{-5}$ kg/(m s), leading to a Reynolds number, $Re = 1.5 \times 10^6$. Wall normal resolutions were chosen to adequately represent the boundary layers on both the wing and tunnel walls. The $k - \omega$ SST RANS turbulence model was employed for the simulations. Due to the complexity of mesh generation, only one mesh with approximately 3 million grid points was generated.

Coarsening is based on the parallel maximal independent set (PMIS) algorithm of Luby [17, 18, 21] allowing for a parallel setup phase. The strength of connection threshold is set to $\theta = 0.25$. Aggressive coarsening is applied on the first two V -cycle levels with multi-pass interpolation and a stencil width of two elements per row. The remaining levels employ M-M extended+i interpolation, with truncation level 0.25 together with a maximum stencil width of two matrix elements per row. The smoother is hybrid block-Jacobi with two sweeps of polynomial Gauss-Seidel applied locally on an MPI rank and then Jacobi smoothing for globally shared degrees of freedom. The coarsening rate for the wing simulation is roughly 4 \times with eight levels in the V -cycle for hypre. Operator complexity C is close to 1.6 indicating more efficient V -cycles with aggressive coarsening, however, an increased number of GMRES iterations

are required compared to standard coarsening. The comparison among ℓ_1 -Jacobi, Gauss-Seidel and the polynomial Gauss-Seidel smoothers is shown in Figure 2.

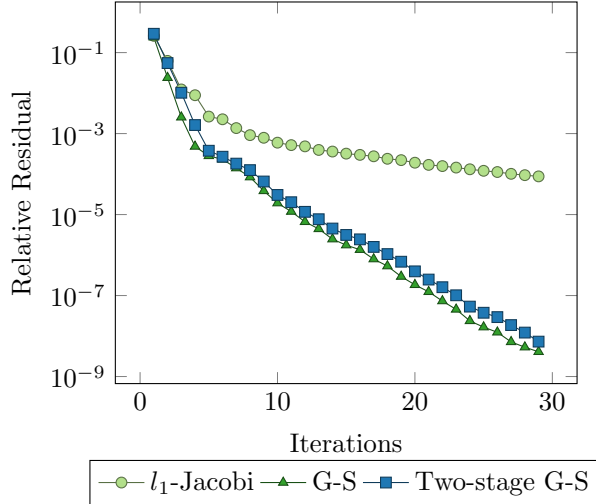


Fig. 2: GMRES+AMG with ℓ_1 -Jacobi, Gauss-Seidel and poly Gauss-Seidel smoothers for a linear system from Nalu-Wind model with dimension $N = 3.1$ million.

In order to evaluate the differences between the direct and iterative triangular solvers employed in the smoother, the compute times for a single GMRES+AMG pressure solve are given in Table 6. The ℓ_1 -Jacobi smoother from hypre is included for comparison. Both the CPU and GPU times are reported for the NREL Eagle supercomputer with Intel Skylake Xeon CPUs and NVIDIA V100 GPU’s. In all cases, one sweep of Gauss-Seidel and two sweeps of ℓ_1 -Jacobi are employed because the number of sparse matrix-vector multiplies are equivalent in both cases. Either one CPU or GPU was employed in these tests. The time reported corresponds to when the relative residual has been reduced below $1e-5$.

	ℓ_1 -Jacobi	Gauss-Seidel	Poly G-S
CPU (sec)	19.4	12	19.5
GPU (sec)	0.33	3.1	0.30

Table 6: GMRES+AMG compute time. Jacobi, Gauss-Seidel and Poly Gauss-Seidel Smoothers for a linear system from Nalu-Wind model with dimension $N = 3.1$ million.

The timing results indicate the solver time with Gauss-Seidel is lower than when the ℓ_1 Jacobi smoother is employed on the CPU. However, the latter is more computationally efficient on the GPU. Whereas the polynomial Gauss-Seidel smoother leads to the lowest compute times on the GPU and results in a ten times speed-up compared to the smoother that employs a direct triangular solver.

6.2. PeleLM Model. Pressure linear systems are taken from the “nodal projection” component of the time integrator used in PeleLM [37]. PeleLM is an adaptive mesh low Mach number combustion code developed and supported under DOE’s Exascale Computing Program. PeleLM features the use of a variable-density projection scheme to ensure that the velocity field used to advect the state satisfies an elliptic divergence constraint. Physically, this constraint enforces that the resulting flow evolves consistently with a spatially uniform thermodynamic pressure across the domain. A key feature of the model is that the fluid density may vary considerably across the computational domain. Extremely ill-conditioned problems arise for incompressible and reacting flows in the low Mach flow regime, particularly when using cut-cell approaches to complex geometries, where non-covered cells that are cut by the domain boundary can have arbitrarily small volumes and areas. The standard Jacobi and Gauss-Seidel

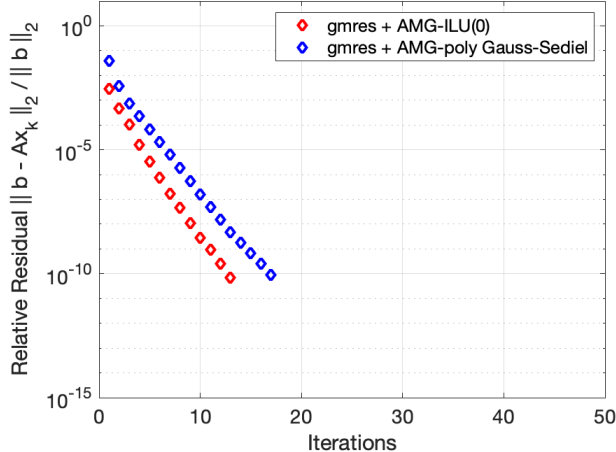


Fig. 3: PeleLM convergence history of GMRES+AMG. Poly Gauss-Seidel and ILU(0) smoothers with iterative triangular solves using three (3) Jacobi iterations. Matrix dimension $N = 1.4$ million.

smoothers are less effective in these cases at reducing the residual error at each level of the C-AMG V -cycle and this can lead to very large iteration counts for the Krylov solver.

The Krylov solver was run with a hybrid V -cycle with ILU smoothing only on the finest level $\ell = 1$, and polynomial Gauss-Seidel on the remaining levels. Iterative Jacobi triangular solvers were employed. One pre- and post-smoothing sweep was applied on all V -cycle levels, except for the coarse level direct solve. The polynomial smoother leads to a slower convergence rate compared to the hybrid and ILU smoothers, which exhibit similar convergence. Because an $A \approx LDU$ factorization is employed in hypre, Ruiz scaling was not required in our numerical experiments. Furthermore, only three Jacobi iterations for L and U were needed to achieve sufficient accuracy to maintain the convergence rate.

Results for the $N = 1.4$ million linear system, representing a cylindrical geometry, are plotted in Figure 3. These results were obtained on the Intel Skylake CPUs and NVIDIA V100 GPUs. “MM-ext+i” interpolation is employed, with a strength of connection threshold $\theta = 0.25$. Because the problem is very ill-conditioned, GMRES achieves the best convergence rates and the lowest NRBE. Iterative triangular solvers were employed in these tests. The convergence histories are plotted for hybrid ILU, and polynomial Gauss-Seidel smoothers in Figure 3. The fastest convergence rate was achieved when the level of fill parameter was set to $lfil = 10$ and with a drop tolerance of $tol = 1 \times 10^{-2}$. The reduction in the relative residual is sufficient for the pressure equation after three GMRES iterations. The ILUT parameters were $droptol = 1e-2$ and $lfil = 5$.

Finally, the compute times of the GMRES+AMG solver, using either direct or iterative triangular solvers in the ILU smoother, are compared. The compute times for a single pressure solve are given in Table 7. The ILU(0) and Gauss-Seidel smoothers are included for comparison. Both the CPU and GPU times are reported. In all cases, one Gauss-Seidel and one ILU sweep are employed. The solver time reported corresponds to when the relative residual has been reduced below $1e-5$.

	Gauss-Seidel	Poly G-S	ILUT direct	ILUT Jacobi	ILU(0) Jacobi
CPU (sec)	9.2	9.6	4.3	6.9	6.8
GPU (sec)	4.5	0.13	0.17	0.11	0.086

Table 7: GMRES+AMG compute time. Gauss-Seidel, poly Gauss-Seidel, and ILU Smoothers for a linear system from PeleLM with dimension $N = 1.4$ million.

Both the CPU and GPU timing results for the PeleLM nodal projection pressure solver are compared in Table 7. First, let us consider the CPU compute times for a single solve. The results indicate that

the solver time using the hybrid V -cycle with an ILU smoother on the first level, with a direct solver for the L and U factors, is less than when a Gauss-Seidel smoother is applied on all levels. One sweep of the G-S smoother is employed in both configurations. The longer time is primarily due to the higher number of iterations required in this case. The ILU smoother with iterative triangular solvers is the more efficient approach on the GPU. Despite only three (3) sparse matrix-vector (SpMV) products for the Jacobi iterations to solve the L and U triangular systems, the computational speed of the GPU for the SpMV kernel is more than sufficient to overcome the direct sparse triangular solve.

To further explore the parallel strong-scaling behaviour of the iterative and direct solvers within the ILU smoothers, the GMRES+AMG solver was employed to solve a PeleLM linear system of dimensions $N = 11$ million. The LDU form of the incomplete factorization with row scaling was again employed and ten (10) Jacobi iterations provide sufficient smoothing for this much larger problem. The convergence histories are displayed in Figure 4. The linear system solver was tested on the ORNL Summit Supercomputer using six NVIDIA Volta V100 GPUs per node, scaling out to 192 nodes, or 1152 GPUs. Most notably, the solver with iterative Jacobi triangular solves achieves a ten times faster compute time compared to the direct triangular solver as displayed in Figure 5.

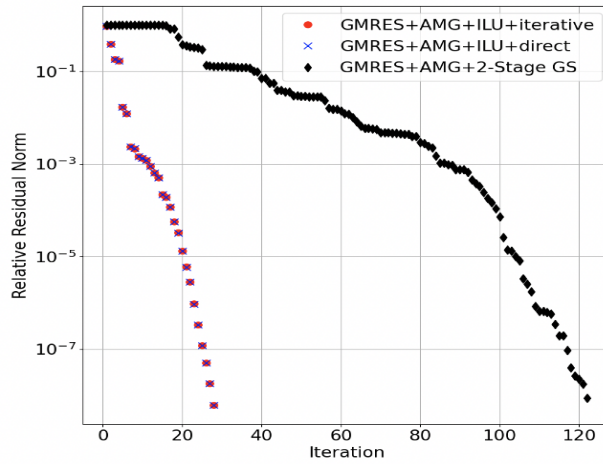


Fig. 4: Hypre-BoomerAMG results. Convergence histories of GMRES+AMG with polynomial two-stage Gauss-Seidel and ILU(0) smoothers using direct and iterative triangular solves for a linear system from PeleLM with dimension $N = 11$ million.

7. Conclusions. We have shown how Neumann series play an important role in a low-synch formulation of the MGS-GMRES algorithm as well as both polynomial Gauss-Seidel and ILU smoothers for an AMG preconditioner. These algorithms are well-suited to GPU accelerators because they rely on matrix-vector products. Indeed, the MGS projection step and the AMG smoother can both be accelerated by a factor of 25–50 \times on current GPU architectures. To a large extent, the loss of orthogonality of the Krylov vectors determines when the solver will converge to a backward stable solution. The loss of orthogonality results elucidated by Paige and Strakoš [7] imply that the strictly lower triangular matrix L_k , appearing in the correction matrix T_k , remains small in the Frobenius norm and thus $T_k = I - L_k$ is sufficient for convergence when $\|L_k\|_F^p = \mathcal{O}(\varepsilon^p)\kappa_F^p(B)$, and $p > 1$. The Neumann series is a finite sum because L_k is strictly lower triangular and nilpotent.

The iteration matrices for polynomial Gauss-Seidel and ILU smoothers may be expressed as Neumann series. When higher-order terms are included, rapid convergence is achieved for GMRES-AMG applied to the incompressible Navier-Stokes equations pressure solver. A block-Jacobi type smoother is applied within each parallel process (MPI rank) by hybrid smoothers for the local block diagonal matrices. The approximate minimum degree (amd) matrix re-ordering combined with an LDU factorization leads to rapid convergence of the Jacobi iterations for the triangular factors L and U for slightly non-symmetric linear systems. The Krylov solver was found to converge faster and take less compute

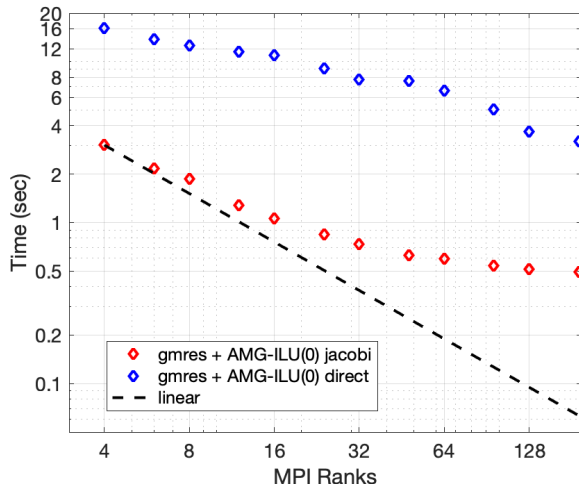


Fig. 5: Hypre-BoomerAMG strong-scaling results. GMRES+AMG with ILU(0) smoothers using direct and iterative triangular solves for a linear system from PeleLM with dimension $N = 11$ million.

time when AMG with ILU(0) smoothers and iterated triangular solves were then employed. We conjecture that re-orderings which preserve structural symmetry of the matrix also lead naturally to a small departure from normality $dep(U)$ for the triangular factors arising from an LDU factorization.

Pressure continuity problems from the PeleLM adaptive mesh combustion model was also examined. GMRES-AMG solver convergence is essentially identical for the standard and polynomial Gauss-Seidel smoothers. However, the run-time on a many-core GPU accelerator drops in comparison with the conventional Gauss-Seidel smoother and remains lower even when a Jacobi smoother is applied. The PeleLM nodal pressure projection linear systems were highly ill-conditioned due to the variable density across the computational domain combined with the mesh geometry. A sufficient reduction in the norm-wise relative backward error was achieved using an ILU smoother with LDU factorization and iterative solution of the triangular systems. Despite the need for $\mathcal{O}(10)$ Jacobi iterations for these sparse triangular solves, the sparse matrix-vector product (SpMV) kernel for the GPU is much faster than the direct triangular solver, resulting in a ten times faster compute time. We plan to explore the fixed-point iteration algorithms of Chow and Patel [26] and also Anzt et al. [38] to compute the ILU(0) and ILUT factorizations in order to reduce the C-AMG set-up costs.

Acknowledgment. Funding was provided by the Exascale Computing Project (17-SC-20-SC). The National Renewable Energy Laboratory is operated by Alliance for Sustainable Energy, LLC, for the U.S. Department of Energy (DOE) under Contract No. DE-AC36-08GO28308. A portion of this research used resources of the Oak Ridge Leadership Computing Facility, which is a DOE Office of Science User Facility supported under Contract DE-AC05-00OR22725 and using computational resources at NREL, sponsored by the DOE Office of Energy Efficiency and Renewable Energy.

REFERENCES

- [1] C. C. Paige, M. Rozložník, Z. Strakoš, Modified Gram-Schmidt (MGS), least squares, and backward stability of MGS-GMRES, *SIAM Journal on Matrix Analysis and Applications* 28 (1) (2006) 264–284.
- [2] R. D. Falgout, J. E. Jones, U. M. Yang, The design and implementation of hypre, a library of parallel high performance preconditioners, in: A. M. Bruaset, A. Tveito (Eds.), *Numerical Solution of Partial Differential Equations on Parallel Computers*, Springer Berlin Heidelberg, Berlin, Heidelberg, 2006, pp. 267–294.
- [3] Y. Saad, M. H. Schultz, GMRES: A generalized minimal residual algorithm for solving nonsymmetric linear systems, *SIAM Journal on scientific and statistical computing* 7 (3) (1986) 856–869.
- [4] K. Swirydowicz, J. Langou, S. Ananthan, U. Yang, S. Thomas, Low synchronization Gram-Schmidt and generalized minimal residual algorithms, *Numerical Linear Algebra with Applications* 28 (2020) 1–20.
- [5] J. W. Ruge, K. Stüben, Algebraic multigrid, in: *Multigrid methods*, SIAM, 1987, pp. 73–130.

- [6] A. Sharma, S. Ananthan, J. Sitaraman, S. Thomas, M. A. Sprague, Overset meshes for incompressible flows: On preserving accuracy of underlying discretizations, *Journal of Computational Physics* 428 (2021) 1–29.
- [7] C. C. Paige, Z. Strakoš, Residual and backward error bounds in minimum residual Krylov subspace methods, *SIAM Journal on Scientific and Statistical Computing* 23 (6) (2002) 1899–1924.
- [8] D. Bielich, J. Langou, S. Thomas, K. Świrydowicz, I. Yamazaki, E. Boman, Low-synch Gram-Schmidt with delayed reorthogonalization for Krylov solvers, *Parallel Computing* (2021).
- [9] A. Ruhe, Numerical aspects of Gram-Schmidt orthogonalization of vectors, *Linear Algebra and its Applications* 52 (1993) 591–601.
- [10] P. Muldowney, R. Li, S. Thomas, S. Ananthan, A. Sharma, A. Williams, J. Rood, M. A. Sprague, Preparing an incompressible-flow fluid dynamics code for exascale-class wind energy simulations, in: *Proceedings of the ACM/IEEE Supercomputing 2021 Conference*, ACM, 2021.
- [11] E. Chow, Y. Saad, Experimental study of ILU preconditioners for indefinite matrices, *Journal of Computational and Applied Mathematics* 86 (1997) 387–414.
- [12] S. Thomas, A. Carr, P. Muldowney, K. Świrydowicz, M. Day, ILU smoothers for C-AMG with scaled triangular factors, arXiv preprint arXiv:2111.09512 (2021).
- [13] H. Anzt, E. Chow, J. Dongarra, Iterative sparse triangular solves for preconditioning, in: *European conference on parallel processing*, Springer, 2015, pp. 650–661.
- [14] P. Henrici, Bounds for iterates, inverses, spectral variation and fields of values of non-normal matrices, *Numerische Mathematik* 4 (1) (1962) 24–40.
- [15] W. Oettli, W. Prager, Compatibility of approximate solutions of linear equations with given error bounds for coefficients and right hand sides, *Numerische Mathematik* 6 (1964) 405–409.
- [16] J. L. R. and J. Gaches, On the compatibility of a given solution with the data of a linear system, *Journal of the ACM* 14 (1967) 543–548.
- [17] H. De Sterck, U. Meier-Yang, J. J. Heys, Reducing complexity in parallel algebraic multigrid preconditioners, *SIAM Journal on Matrix Analysis and Applications* 27 (4) (2006) 1019–1039.
- [18] M. Luby, A simple parallel algorithm for the maximal independent set problem, *SIAM Journal on Computing* 15 (1986) 1036–1053.
- [19] K. Stüben, Algebraic multigrid (AMG): an introduction with applications, in: U. Trottenberg, A. Schuller (Eds.), *Multigrid*, Academic Press, Inc., USA, 2000.
- [20] T. Manteuffel, S. McCormick, M. Park, J. Ruge, Operator-based interpolation for bootstrap algebraic multigrid, *Numerical Linear Algebra with Applications* 17 (2-3) (2010) 519–537.
- [21] H. De Sterck, R. D. Falgout, J. W. Noltling, U. Meier-Yang, Distance-two interpolation for parallel algebraic multigrid, *Numerical Linear Algebra with Applications* 15 (2-3) (2008) 115–139.
- [22] R. Li, B. Sjøgreen, U. Meier-Yang, A new class of AMG interpolation operators based on matrix matrix multiplications, To appear *SIAM Journal on Scientific Computing* (2020).
- [23] U. Meier-Yang, On long-range interpolation operators for aggressive coarsening, *Numerical Linear Algebra with Applications* 17 (2-3) (2010) 453–472.
- [24] R. D. Falgout, R. Li, B. Sjøgreen, U. Meier-Yang, Porting *hypre* to heterogeneous computer architectures: Strategies and experiences, submitted to *Parallel Computing* (2020).
- [25] A. H. Baker, R. D. Falgout, T. V. Kolev, U. M. Yang, Multigrid smoothers for ultraparallel computing, *SIAM J. Sci. Comput.* 33 (2011) 2864–2887.
- [26] E. Chow, A. Patel, Fine-grained parallel incomplete LU factorization, *SIAM Journal on Scientific Computing* 37 (2) (2015) C169–C193.
- [27] M. Eiermann, **Fields of values and iterative methods**, *Linear Algebra and its Applications* 180 (1993) 167–197. doi:[https://doi.org/10.1016/0024-3795\(93\)90530-2](https://doi.org/10.1016/0024-3795(93)90530-2). URL <https://www.sciencedirect.com/science/article/pii/0024379593905302>
- [28] R. A. Horn, C. R. Johnson, *Matrix analysis*, Cambridge university press, 2012.
- [29] P. A. Knight, D. Ruiz, B. Uçar, A symmetry preserving algorithm for matrix scaling, *SIAM Journal on matrix analysis and applications* 35 (3) (2014) 931–955.
- [30] I. C. Ipsen, A note on the field of values of non-normal matrices, Tech. rep., North Carolina State University. Center for Research in Scientific Computation (1998).
- [31] L. Elsner, M. Paardekooper, On measures of nonnormality of matrices, *Linear Algebra and its Applications* 92 (1987) 107–123.
- [32] L. Trefethen, M. Embree, *The behavior of nonnormal matrices and operators*, *Spectra and Pseudospectra* (2005).
- [33] M. Asllani, R. Lambiotte, T. Carletti, Structure and dynamical behavior of non-normal networks, *Sci. Adv.* 4 9403 (2018).
- [34] A. George, J. Liu, *Computer Solution of Large Sparse Positive Definite Matrices*, Prentice Hall, 1981.
- [35] P. R. Amestoy, T. A. Davis, I. S. Duff, An approximate minimum degree ordering algorithm, *SIAM Journal on Matrix Analysis and Applications* 17 (4) (1996) 886–905.
- [36] A. George, Nested dissection of a regular finite element mesh, *SIAM Journal on Numerical Analysis* 10 (2) (1973) 345–363.
- [37] A. Nonaka, J. B. Bell, M. S. Day, A conservative, thermodynamically consistent numerical approach for low Mach number combustion. I. Single-level integration, *Combust. Theor. Model.* 22 (1) (2018) 156–184.
- [38] H. Anzt, T. Ribizel, G. Flegar, E. Chow, J. Dongarra, ParILUT - a parallel threshold ILU for GPUs, in: *International Conference on Parallel Processing and Applied Mathematics*, Springer, 2011, pp. 133–142.